ChemPubSoc Europe

DOI: 10.1002/open.201900103

Open Access ChemistryOPEN Full Papers

Modulation of Conformational Preferences of Heteroaromatic Ethers and Amides through Protonation and Ionization: Charge Effect

Wenshuai Dai,[a, b] Zhe Zhang,[a, b] and Yikui Du*[a]

Multiple approaches reveal the strong effects of a positive charge introduced by protonation or ionization on the conformation of *o*-heteroaromatic ethers and amides. The ethers and amides containing an *ortho*-N heteroatom are *syn*-preferring while those containing an *ortho*-O or *ortho*-S heteroatom are mostly *anti*-preferring. However, for all the monocyclic *o*-heteroaromatic ethers and amides, the protonated ones are all *anti*-preferring while the ionized ones are all *syn*-preferring. Interestingly, although both the protonation and ionization introduce a positive charge, they have such different effects on molecular conformation, very informative for understanding the origin of conformational preferences. Detailed analysis shows that the population of the introduced positive charge dictates the conformational preferences via electrostatic and orbital interactions. Compared to *ortho*-heteroatoms, *meta*-heteroatoms have weaker effect on conformational preference. Achieved by complete inductive method, the regularity of conformational preferences and switching provides easy ways to modulate conformers (by pH or redox), and makes this kind of ether or amide bond a conformational hinge applicable to design of functional molecules (drugs and materials) and modulation of molecular biological processes.

1. Introduction

Conformational preference and switching are of theoretical[1–6] and practical[7–10] importance. The origin of conformational preference and internally rotational barrier has long been related to the steric,[2] quantum[3] and electrostatic effects.[5,6,11] And there are still controversies about which factor is more important.[5] Heterocycles are usually important components of natural compounds[12,13] and functional molecules[14,15] and can influence molecular conformation and properties. Since the heterocyclic ring adjacent to an ether oxygen[11] or amide[6] can determine molecular conformation, they can be used as heterocyclic hinges to orient a chain in conformational space.[7,16] In drug design, this kind of heterocyclic hinge has been used as switch between agonist and antagonist ligand conformations.[7] Strong conformational preferences of 2-methoxyheteroarenes induced by electron pair repulsion make the heteroaromatic ether bond a potential conformational switch.[11] However, information and knowledges on the conformation of heteroaromatic molecules are still scattering. A generalized regularity of conformational preferences and switching can be used for molecular design, especially for the functional molecules with special conformational structure.

For the water- and oxygen-rich system of atmosphere, hydrosphere, geosphere and biosphere on earth, the pH- and redox-related reactions are of great importance, which are taught in early stage of chemical education. The pH- and redox-triggered conformational switching or stabilization may play crucial roles. For example, the pH-triggered conformational switch of heteroaromatic lipids can control the channels on membrane.[17] The ionization/oxidation-induced conformational switching of some aromatic compounds is also found.[18,19] If the protonation or ionization can modulate the conformation of heteroaromatics, the heterocyclic hinges can operate by pH or redox. Since both the protonation and ionization introduce one positive charge into the molecule, the effect of the positive charge on stability of molecular conformers will provide information helpful for understanding the origin of conformational preferences.

To explore the effect of charge on the molecular conformation, we investigated the effect of protonation and ionization on conformational preferences of all the *o*-heteroaromatic ethers and amides by calculating energy differences between *syn* and *anti* conformers. The conformational switching caused by protonation and ionization are discussed in detail.

[a] *Dr. W. Dai, Dr. Z. Zhang, Prof. Y. Du*
Beijing National Laboratory of Molecular Science, State Key laboratory of Molecular Reaction Dynamics,
Institute of Chemistry, Chinese Academy of Sciences
Beijing, 100190 Beijing (PR China)
E-mail: ydu@iccas.ac.cn
[b] *Dr. W. Dai, Dr. Z. Zhang*
School of Chemical Engineering,
University of Chinese Academy of Sciences,
Beijing, 100049, P. R. China

Supporting information for this article is available on the WWW under https://doi.org/10.1002/open.201900103

©2019 The Authors. Published by Wiley-VCH Verlag GmbH & Co. KGaA. This is an open access article under the terms of the Creative Commons Attribution Non-Commercial NoDerivs License, which permits use and distribution in any medium, provided the original work is properly cited, the use is non-commercial and no modifications or adaptations are made.

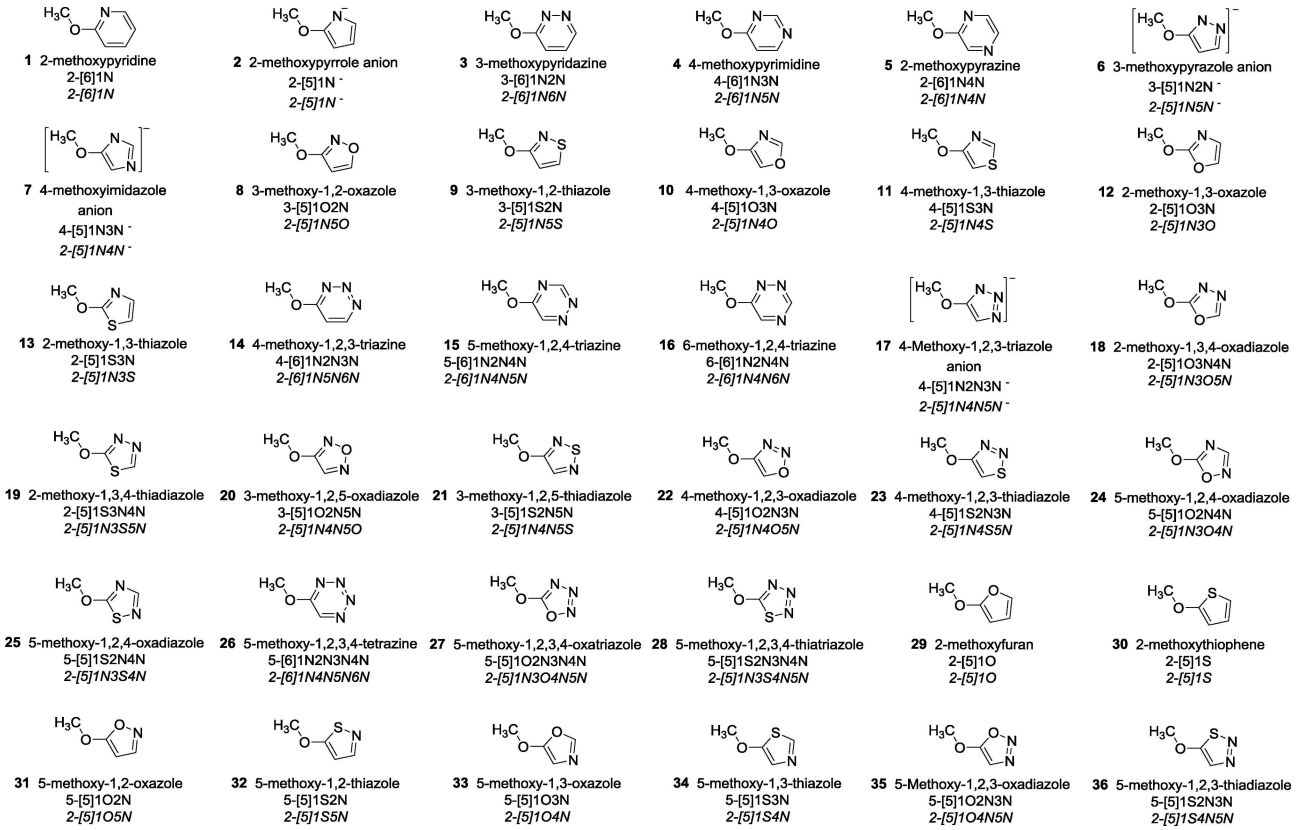

Figure 1. The *syn* conformers of *o*-methoxyheteroarenes. The standard nomenclature is given at first. For convenience, the corresponding abbreviation is employed to represent the nomenclature and structure of each compound, where the first digit marks the position of OCH_3 on the ring and the second digit in square brackets, [5] or [6], marks the five- or six-membered ring, followed by digits and symbols corresponding to the position of heteroatoms on the ring. Finally, the re-defined abbreviations setting the position of OCH_3 as *ortho* are displayed in *italic* type.

2. Results

2.1. Conformational Preferences of *o*-Heteroaromatic Ethers: Effects of Protonation and Ionization

Figure 1 depicts the *syn* conformers of all kinds of the monocyclic *o*-methoxyheteroarenes having *ortho*-heteroatom effect (compounds **1**–**36**), which are calculated at ωB97XD/cc-pVTZ[20,21] level with Gaussian 09.[22] Note that the *syn* or *anti* conformers are defined according to the orientation of methyl group with respect to the in-plane lone pair electrons on the *ortho*-heteroatom. For those containing more than one *ortho*-heteroatoms, according to the conventional rules, the priority has the largest atom (higher atomic number) in determining the substituent position. However, since the effects of *ortho*-heteroatom on conformational preferences have the order N > O or S, the *ortho*-position of each compound is re-defined accordingly. Table 1 lists the calculated energy differences between *syn* and *anti* conformers of *o*-methoxyheteroarenes having *ortho*-heteroatom effect. It can be seen that, for all the ethers having an *ortho*-N heteroatom **1**–**28**, the *syn* conformers have lower potential energy and are more stable than the corresponding anti ones, suggesting the *syn* preferences.[11,23] This means that the *ortho*-N heteroatom has a strong *syn*-preferring effect, which is also verified by performing resonance enhanced two-photon ionization experiments on *2-[6]-1N* **1** (Figure 2) and the cationic spectroscopy.[18] On the other hand, for ethers having an *ortho*-O or *ortho*-S but no *ortho*-N (ethers **29**–**36**), most have *anti* preferences (ethers **29**–**34**, **36**), except

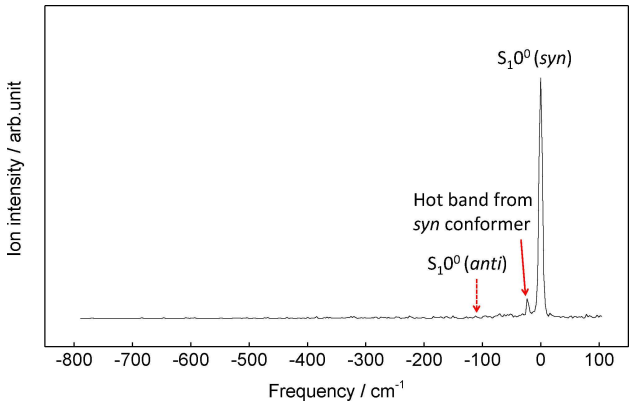

Figure 2. The one-color resonance enhanced two-photon ionization (1C–R2PI) spectrum of 2-[6]-1N **1**. The $S_1 \leftarrow S_0$ electronic transition energy (E_1) of *syn* conformer is set as 0 cm^{-1}. The E_1 of anti conformer is predicted by CIS/cc-pVTZ calculations (the electronic energy corrected by EOM-CCSD/cc-pVTZ) at about 107 cm^{-1} lower than that of the *syn* conformer, which is not observed in the 1C-R2PI spectrum, indicating too low population to be detected. The observed bands are assigned based on the cationic spectroscopy.[18]

© 2019 The Authors. Published by Wiley-VCH Verlag GmbH & Co. KGaA

Table 1. The conformational preferences and rotational barriers in different states (in kcal/mol).[a]

Numbers	Compounds[b]	ΔE[c]	ΔE (H$^+$)[d]	ΔE (−e)[e]	E_B[f]	E_B (−e)[g]	ΔE_B[h]
1	*2-[6]1N*	**4.08**	*−3.23*	**6.22**	7.69	19.77	12.08
2	*2-[5]1N*$^-$	**1.68**	*−3.70*[i]	**3.91**	2.88	10.98	8.10
3	*2-[6]1N6N*	**4.96**	*−1.65*	**2.84**	8.04	8.35	0.31
4	*2-[6]1N5N*	**3.96**	*−3.34*	**3.11**	8.90	11.19	2.29
5	*2-[6]1N4N*	**4.06**	*−2.77*	**6.21**	7.53	15.91	8.38
6	*2-[5]1N5N*$^-$	**2.24**	*−2.96*	**3.13**	3.31	11.70	8.39
7	*2-[5]1N4N*$^-$	**1.06**	*−4.18*[i]	**4.43**	2.68	11.24	8.56
8	*2-[5]1N5O*	**3.61**	*−1.68*	**1.14**	5.88	15.44	9.56
9	*2-[5]1N5S*	**4.23**	*−1.81*	**4.61**	6.79	17.86	11.07
10	*2-[5]1N4O*	**0.53**	*−4.47*	**5.09**	3.88	16.53	12.65
11	*2-[5]1N4S*	**0.84**	*−4.59*	**4.80**	4.46	16.80	12.34
12	*2-[5]1N3O*	**3.22**	*−3.03*	**2.42**	5.54	13.61	8.07
13	*2-[5]1N3S*	**3.34**	*−2.78*	**4.29**	6.09	15.14	9.05
14	*2-[6]1N5N6N*	**4.34**	*−1.70*	**3.53**	9.05	11.21	2.16
15	*2-[6]1N4N5N*	**4.36**	*−2.47*	**4.40**	9.28	12.55	3.27
16	*2-[6]1N4N6N*	**4.95**	*−1.02*	**3.44**	7.95	8.52	0.57
17	*2-[5]1N4N5N*$^-$	**1.65**	*−3.01*	**4.00**	3.01	12.27	9.26
18	*2-[5]1N3O5N*	**3.77**	*−2.28*	**2.03**	5.60	14.21	8.61
19	*2-[5]1N3S5N*	**3.97**	*−1.92*	**3.43**	6.12	13.28	7.16
20	*2-[5]1N4N5O*	**3.68**	*−0.86*	**2.99**	5.76	16.56	10.80
21	*2-[5]1N4N5S*	**3.98**	*−1.26*	**5.17**	6.61	17.56	10.95
22	*2-[5]1N4O5N*	**0.84**	*−3.08*	*[j]	3.25	*[j]	*[j]
23	*2-[5]1N4S5N*	**1.37**	*−3.18*	**3.46**	4.32	14.37	10.05
24	*2-[5]1N3O4N*	**2.27**	*−4.31*	**1.43**	6.54	14.71	8.17
25	*2-[5]1N3S4N*	**2.89**	*−3.05*	**4.93**	7.29	16.40	9.11
26	*2-[6]1N4N5N6N*	**4.83**	*−0.75*	*[j]	9.54	*[j]	*[j]
27	*2-[5]1N3O4N5N*	**2.45**	*−4.04*	**0.08**	6.99	14.54	7.55
28	*2-[5]1N3S4N5N*	**3.25**	*−2.31*	**3.62**	7.44	8.27	0.83
29	*2-[5]1O*	*−1.14*	*−6.82*[i]	**1.58**	1.26	12.25	10.99
30	*2-[5]1S*	*−0.92*	*−4.45*[i]	**0.62**	1.21	12.51	11.30
31	*2-[5]1O5N*	*−0.16*	*−5.49*[i]	**3.47**	3.40	15.35	11.95
32	*2-[5]1S5N*	*−0.47*	*−3.55*	**0.75**	3.15	14.75	11.60
33	*2-[5]1O4N*	*−1.37*	*−6.85*[i]	**2.03**	0.91	12.99	12.08
34	*2-[5]1S4N*	*−1.13*	*−4.3*[i]	**1.64**	1.01	13.42	12.41
35	*2-[5]1O4N5N*	**0.15**	*[j]	*[j]	4.20	*[j]	*[j]
36	*2-[5]1S4N5N*	*−0.36*	*[j]	**2.40**	3.31	*[j]	*[j]

[a] Calculated at ωB97XD/cc-pVTZ level. [b] The protonated and ionized ethers are identified by alphanumeric numbering, which are not displayed in this table. For example, the protonated and ionized 2-[6]1N are defined as **1a** and **1b**, respectively. [c] Energy differences for the ethers before ionization, $\Delta E = E_{anti} - E_{syn}$, the values marked in **bold** and *italic* represent *syn* and *anti* preferences, respectively. [d] Mono-protonation at the *ortho*-N heteroatom of the ethers in group I, while the *ortho*-O or S atom is protonated for the ethers in group II. [e] Energy differences for the ionized ethers, $\Delta E(-e) = E_{anti}(-e) - E_{syn}(-e)$. [f] The rotational barriers of OCH_3 group for ethers before ionization. [g] The rotational barriers of OCH_3 group for ethers after ionization. [h] $\Delta E_B = E_B(-e) - E_B$. [i] The values estimated by single point energy. [j] Unstable. Data are unavailable due to the failed convergence during self-consistent field (SCF) or optimization steps.

for the *2-[5]1O4N5N* **35** (with very weak *syn* conformational preference). This means that the *ortho*-O or *ortho*-S heteroatom has a relatively weak *anti*-preferring effect, which may be affected by other factors. The *o*-heteroatoms play an imperative role in determining the conformational preferences, while the heteroatoms on other positions have slight effects. So, based on the conformational preferences, all the monocyclic *o*-heteroaromatic ethers can be divided into two groups. The ethers **1**–**28** having one *ortho*-N heteroatom belong to group I, which prefer *syn* conformers. The ethers **29**–**36** having only one heteroatom (O or S) at the double *ortho*-positions belong to group II, which mainly prefer *anti* conformers. Chein and Corey[11] observed the *syn* preferring *ortho*-N and the *anti* preferring *ortho*-O or *ortho*-S heteroatom effects in studying ethers **1**, **3**, **12**, **13**, **29** and **32**, but, by checking all the *o*-methoxyheteroarenes, we found an exception, the *syn* preference of *2-[5]1O4N5N* **35**. For the *o*-methoxyheteroarenes, the *ortho*-heteroatom effects on conformational preferences derived by complete induction method here can be considered as a kind of propensity regularity, which is convenient for application.

For ethers having both *ortho*-N (preferring *syn* conformer) and *ortho*-O or S heteroatoms (preferring *anti* conformer), due to the pull-push mechanism, there might be an additive effect on conformational preferences. This kind of cooperating effect is confirmed by comparing the data for ethers containing both *ortho*-N and *ortho*-O or S heteroatoms with that of ethers containing only one *ortho*-heteroatom (N, O or S). For example, the conformational preference of *2-[5]1N3O* **12** is determined to be 3.22 kcal/mol, remarkably higher than the 1.68 kcal/mol for 2-[5]1N$^-$ **2** and 0.53 kcal/mol for *2-[5]1N4O* **10**, showing the existence of additive effect, although the effects of charge and *meta*-heteroatom can't be excluded. It can be seen that, not only the *2-[5]1N4O* **10**, but also *2-[5]1N5N*$^-$ **6** and *2-[5]1N4S* **11** have weaker *syn* preferences compared to the molecules **1**, **3**, **4**, **5** containing six-membered ring. Probably the *meta*-heteroatom effects play an important role. For ethers having two *ortho*-N heteroatoms **37**–**49** (Figure S1), effects of *meta*-heteroatoms on conformational preferences should be considered, which seems irregular (Table S1).

Conformational modulation is usually based on conformational switching. It is reported[24,25] that the conformational preferences can be affected by protonation. Figure 3 (a) displays the potential curves of *2-[6]1N* **1** and its conjugate acid, *2-[6]1NH*$^+$ **1a**. For the neutral *2-[6]1N* **1**, the energy of *anti* conformer is 4.08 kcal/mol higher than that of the *syn* one, indicating a *syn* preference. While for *2-[6]1NH*$^+$ **1a**, the energy difference between the two conformers is determined to be −3.23 kcal/mol and a strong *anti* preference is observed. Even for the ether having only one stable conformer (ethers **50**–**53**, Figure S2), the *anti* preferences can also be found after *ortho*-N protonation (Table S2). The potential curves for other ethers **2**–**28** in group I are given in the Figures S3 and S4. It is demonstrated that, although the neutral or anionic *ortho*-N remarkably prefer *syn* conformers, the protonated *ortho*-N prefers the *anti* ones. This means that, for the ethers containing *ortho*-N heteroatom, the conformational preferences can be modulated through protonation or deprotonation on the *ortho*-N heteroatom. For the ethers of group II, as shown in Table 1, the *anti* preferences of ethers only having *ortho*-O or S heteroatom can be observed before and after the protonation, and the *syn* conformers of the protonated species are nonplanar[26] and relatively unstable. So, it can be concluded that, for all the monocyclic *o*-heteroaromatic ethers, the protonation on *o*-heteroatom gives *anti* preferences. Addition-

© 2019 The Authors. Published by Wiley-VCH Verlag GmbH & Co. KGaA

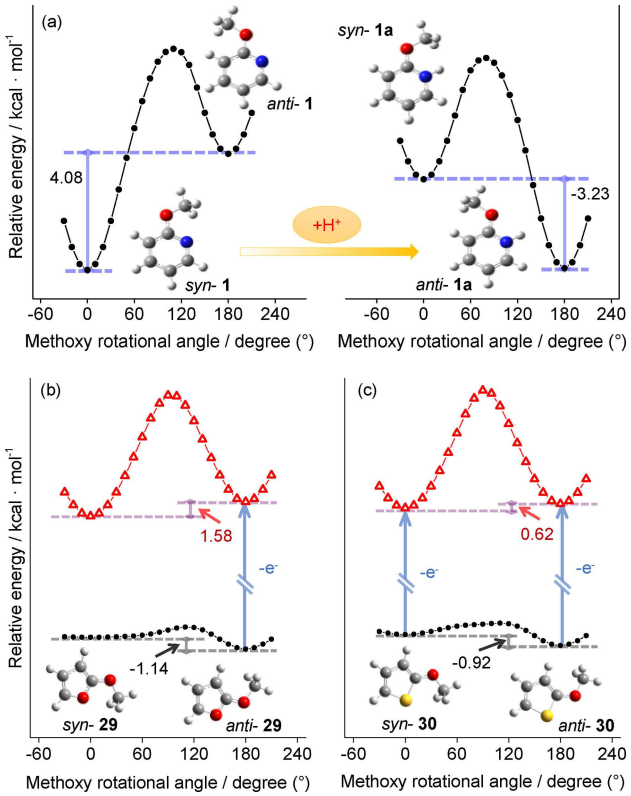

Figure 3. The switching of conformational preference of (a) 2-[6]1N **1** upon protonation, (b) 2-[5]1O **29** upon ionization, and (c) 2-[5]1S **30** upon ionization.

ally, the *anti* preferences of ethers in group II are enhanced by protonation (data for compounds *2-[5]1OH4N5N*$^+$ **35a** and *2-[5]1SH4N5N*$^+$ **36a** are unavailable due to the failed convergence in optimization steps), and most of protonated ethers in group I & II have strong *anti* preferences (> 2.0 kcal/mol), which might be useful for molecular design.

For the ethers containing two or more heteroatoms, the *ortho*-heteroatom is not necessarily the one with strongest basicity, and practically the protonation of all heteroatoms could be considered. Additional calculations show that, for the ethers containing two heteroatoms, the protonation of all the heteroatoms also give the *anti* preferences, suggesting that the protonation on the non-*ortho* heteroatoms has weaker effect than that of *o*-heteroatoms. However, for the ethers containing more than two heteroatoms, application of this conformational modulation through multi-protonation may be difficult. As shown in Table S3, among the fifteen compounds with only one *ortho*-N heteroatom and heteroatoms at other position, ten of them have a conformational switching upon complete protonation, except for *2-[6]1N4N5N* **15**, *2-[6]1N4N6N* **16**, 2-[5]1N4N5O **20**, *2-[5]1N4N5S* **21** and *2-[6]1N4N5N6N* **26**. A possible remedy for the application of mono-protonation triggered conformational switching of those five ethers might be related to the coordination reaction,[27] which can remove the preferred conformer from the chemical equilibrium.

As demonstrated in our previous study,[28] ionization can trigger the conformational switching of some aromatic compounds. The ionization/oxidation effect on the conformational preferences of *o*-methoxyheteroarenes is investigated, as tabulated in Table 1. Firstly, for the compounds of group I, *syn* preferences exist before and after the ionization (data for the ionized state of compounds *2-[5]1N4O5N* **22** and *2-[6]1N4N5N6N* **26** are unavailable due to the failed convergence of optimization steps). Ionization can either enhance or decrease the conformational preferences, but, for application in molecular design, we can find the strong *syn* preference (> 2 kcal/mol) at least in one of two states (before and after ionization) for most ethers of group I, except for the *2-[5]1N4O5N* **22**, which has a weak *syn* preference (0.84 kcal/mol) and is unstable in ionized state. For the ethers with only one *ortho*-O or S heteroatom **29**–**36** (goup II), the *anti* preferences can be changed to *syn* preferences upon ionization, suggesting an ionization-induced conformational switching (as shown in Figure S5). It is to say, although these ethers have *anti* preferences before ionization, they, similar to ethers of group I, have *syn* preferences after ionization. For example, in the ionized state, the *syn 2-[5]1O*$^+$ **29b** and *syn 2-[5]1S*$^+$ **30b** are more stable than the *anti* conformers (Figures 3(b) and (c)). Marked with conformational distributions (data for compounds *2-[5]1O4N5N*$^+$ **35b** and *2-[5]1S4N5N*$^+$ **36b** are not available), the ionization reactions are exhibited in Figure S6. So, it can be concluded that, for all the studied ethers, the ionized or oxidized ones have syn preferences. Additionally, enhancement of conformational preferences upon ionization (Figure S7) is observed for those ethers having weak *syn* preferences (< 1 kcal/mol), except for *2-[5]1N4O5N* **22** that is unstable in the ionized state.

It must be noted that, for the effect of protonation and ionization/oxidation as shown in Table 1, the exceptions which are unstable in the protonated or ionized states only occur for some ethers containing more than two heteroatoms. These ethers are rare compounds and cannot be seen so often in literature, and they are usually not available for use. Having typical effect of protonation and ionization/oxidation, the strong conformational preferences of ethers having one or two heteroatoms are easy applicable and recommended.

The *syn-anti* interconversion barriers are summarized in the last three columns of Table 1, which are remarkably increased upon ionization, due to the increased p-π* conjugation between OCH_3 and ring in the ionized state. For the ionization-triggered conformational switching, excess energy is needed to overcome the higher barrier. Otherwise the conformation will keep as before the ionization. Although it might be a difficulty for the application of the conformational modulation by ionization, it seems that we can take advantage of the higher barriers for the preparation of non-classical conformers. Detailed discussions are shown in the Supporting Information as Figure S8.

© 2019 The Authors. Published by Wiley-VCH Verlag GmbH & Co. KGaA

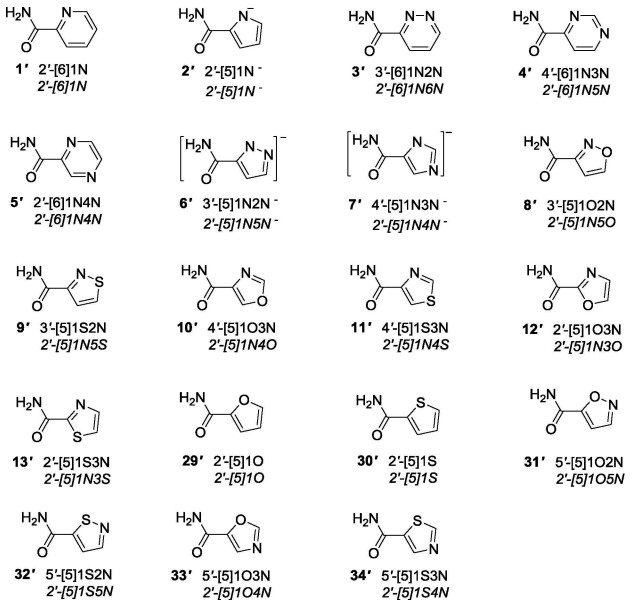

Figure 4. The *syn* conformers of *o*-heteroaromatic amides containing one or two heteroatoms.

2.2. Conformational Preferences of *o*-Heteroaromatic Amides: Effect of Protonation and Ionization

For other heteroaromatic compounds like amides, some of which have recently been explored as drugs,[6,7] the effect of protonation and oxidation on their conformational preferences are similar to that of heteroaromatic ethers. For the amides containing one or two heteroatoms (Figure 4), all the protonated ones are *anti*-preferring, while all the ionized ones are *syn*-preferring, as shown in Table 2. Interestingly, although both protonation and ionization introduce a positive charge, they have such different effects on conformational preferences. Note that, for the amides, the *syn*-preference of *ortho*-N and *anti*-preference of *ortho*-S are similar to those of ethers, however, unlike the *anti*-preference of ethers containing *ortho*-O, the *syn*-preference is found for amides containing *ortho*-O. Additionally, similar to the ethers, there are also several anomalies among the data for the amides in Table 2, such as the small values ($<$ 1 kcal/mol) for energy differences, and the unavailable data due to the failed convergence during the self-consistent field (SCF) or geometrical optimization processes. To confirm the anomalies in Tables 1 and 2 obtained at ωB97XD/cc-pVTZ level, two more computational methods are employed and the results are tabulated in Table 3. Firstly, the calculations are performed at ωB97XD/6-311++g(d,p) level to investigate whether the anomalies are induced by the basis set. As seen from Table 3, it is found that most of the values are similar to the results calculated with cc-pVTZ basis set. For compounds **27b** and **31**, although the sign of these values are opposite to those results calculated at ωB97XD/cc-pVTZ level, all these values are very small and the conformational populations N_{syn}:N_{anti} approximate 1:1. The conformational energy differences are also calculated by using mp2/6-311++g(d,p),[29] which reveals that the values obtained from mp2 calculations are very similar to those from DFT calculations.

Table 2. The conformational preferences of heteroaromatic amides in different states (kcal/mol).[a]

Groups	Numbers[b]	Compounds[c]	ΔE[d]	ΔE(H^+)[e]	ΔE(−e)[f]
Group I	**1′**	*2′-[6]1N*	**8.84**	*−7.39*	**3.77**[g]
(*ortho*-N)	**2′**	*2′-[5]1N⁻*	**7.44**	*−5.29*	**8.05**
	3′	*2′-[6]1N6N*	**9.90**	*−5.03*	**4.30**
	4′	*2′-[6]1N5N*	**8.51**	*−7.18*	**6.73**[g,h]
	5′	*2′-[6]1N4N*	**7.73**	*−8.29*	**9.40**[g,h]
	6′	*2′-[5]1N5N⁻*	**7.84**	*−4.54*	**8.30**
	7′	*2′-[5]1N4N⁻*	**6.78**	*−5.68*	**7.88**
	8′	*2′-[5]1N5O*	**6.59**	*−4.38*	**0.82**
	9′	*2′-[5]1N5S*	**7.37**	*−5.40*	*[i]
	10′	*2′-[5]1N4O*	**6.94**	*−6.84*	**11.78**[g,h]
	11′	*2′-[5]1N4S*	**7.43**	*−7.02*	**9.83**
	12′	*2′-[5]1N3O*	**3.50**	*−7.60*	**4.31**[g,h]
	13′	*2′-[5]1N3S*	**7.77**	*−5.28*	*[i]
Group II	**29′**	*2′-[5]1O*	**3.44**	*[i]	**4.55**[g,h]
(*ortho*-O or S)	**30′**	*2′-[5]1S*	*−0.07*	*−6.07*	**0.72**
	31′	*2′-[5]1O5N*	**4.36**	*[i]	**10.85**[g,h]
	32′	*2′-[5]1S5N*	*−0.14*	*−5.84*	**0.45**
	33′	*2′-[5]1O4N*	**2.79**	*[i]	*[i]
	34′	*2′-[5]1S4N*	*−0.48*	*−5.35*	**5.46**[g,h]

[a] Calculated at ωB97XD/cc-pVTZ level. [b] The serial number of amides are assigned according to the same way with those of ethers in Table 1. Each number followed by the symbol "′ ". [c] The symbol "′" following the substituent position number represents an amide group instead of the ether group. [d] Energy differences for the amides, $\Delta E = E_{anti} - E_{syn}$, the values marked in **bold** and *italic* represent *syn* and *anti* preferences, respectively. [e] Mono-protonation at the *ortho*-N heteroatom of the compounds in group I, but the *ortho*-O or S atom of the compounds in group II. [f] Energy differences for the ionized amides, $\Delta E(-e) = E_{anti}(-e) - E_{syn}(-e)$. [g] Partial optimization results are obtained by freezing the rotational coordinate of the acylamino at 0°. [h] The values are estimated by single point energy. [i] Unstable. Data are unavailable due to the failed convergence during self-consistent field (SCF) or optimization steps.

As listed in Table 3, the similar results calculated with different methods provide a substantiation for the anomalies observed for the conformational preferences. Particularly, in the neutral ground state, conformational preferences are moderate for the ethers **10**, **11**, **22**, **31**, **35** and **36**, similar to those for the amides **30′**, **32′** and **34′**. For the protonated or ionized molecules, mainly due to the failure of convergence, some data are still unavailable, indicating that these molecules might become unstable upon protonation on *o*-heteroatom or ionization.

In summary, theoretical approaches show that, for *o*-heteroaromatic ethers or amides, the *ortho*-heteroatom dictates conformational preference, with *ortho*-N preferring *syn* but *ortho*-S preferring anti, however, the protonation or ionization gives only *anti* or *syn* preference, respectively.

2.3. Potential Applicatons of the Conformation Modulation by Protonation and Ionization

This simple finding enables easy prediction of conformational preferences under acidification or oxidizing conditions. The pH- and redox-triggered conformational switch can alter the bio-

© 2019 The Authors. Published by Wiley-VCH Verlag GmbH & Co. KGaA

Table 3. The anomalies in conformational preferences of ethers and amides calculated at different levels.[a]

Number	Compounds	ΔE Method 1[b]	Method 2[c]	Method 3[d]	ΔE(+H⁺) Method 1	Method 2	Method 3	ΔE(−e⁻) Method 1	Method 2	Method 3
	Ethers									
10	*2-[5]1N4O*	0.53	0.80	0.66						
11	*2-[5]1N4S*	0.84	1.03	1.28						
20	*2-[5]1N4N5O*				−0.86	−0.93	−1.10			
22	*2-[5]1N4O5N*	0.84	1.19	1.58				Opt failure	Opt failure	Opt failure
26	*2-[6]1N4N5N6N*				−0.75	−0.83	−0.91	Opt failure	Opt failure	SCF failure[h]
27	*2-[5]1N3O4N5N*							0.08	−0.01	Opt failure
31	*2-[5]1O5N*	−0.16	0.16	Im[e]						
35	*5-[5]1O4N5N*	0.15	0.53	0.21	Opt failure[f]	Opt failure	Opt failure	Opt failure	Opt failure	Opt failure
36	*5-[5]1S4N5N*	−0.36	−0.59	Im	Opt failure	Opt failure	Opt failure	2.40	3.04	4.36
	Amides									
9′	*2′-[5]1N5S*							*syn*[i]	*syn*	SCF failure
13′	*2′-[5]1N3S*							*syn*	*syn*	*syn*
29′	*2′-[5]1O*	3.44	3.74	2.87	NH_2–COH^+[g]	NH_2–COH^+	NH_2–COH^+			
30′	*2′-[5]1S*	−0.07	−0.06	−0.74						
31′	*2′-[5]1O5N*	4.36	4.74	3.82	NH_2–COH^+	NH_2–COH^+	NH_2–COH^+			
32′	*2′-[5]1S5N*	−0.14	−0.19	−0.49						
33′	*2′-[5]1O4N*	2.79	3.01	2.25	NH_2–COH^+	NH_2–COH^+	NH_2–COH^+	*syn*	*syn*	SCF failure
34′	*2′-[5]1S4N*	−0.48	−0.49	−1.00						

[a] Anomalies are the small values and failures shown in Tables 1 and 2. [b] ωB97XD/cc-pVTZ method. [c] ωB97XD/6-311++g(d,p) method. [d] mp2/6-311++g(d,p) method. [e] One imaginary frequency is found, which involves out-of-plane motion of OCH_3 group. [f] The failed convergence in the optimization process. [g] The protonation occurred on the O atom of the acylamino ($CONH_2$) instead of the *o*-heteroatom on the ring. [h] Failed SCF convergence. [i] Only *syn* conformer is obtained even the input structure is *anti*.

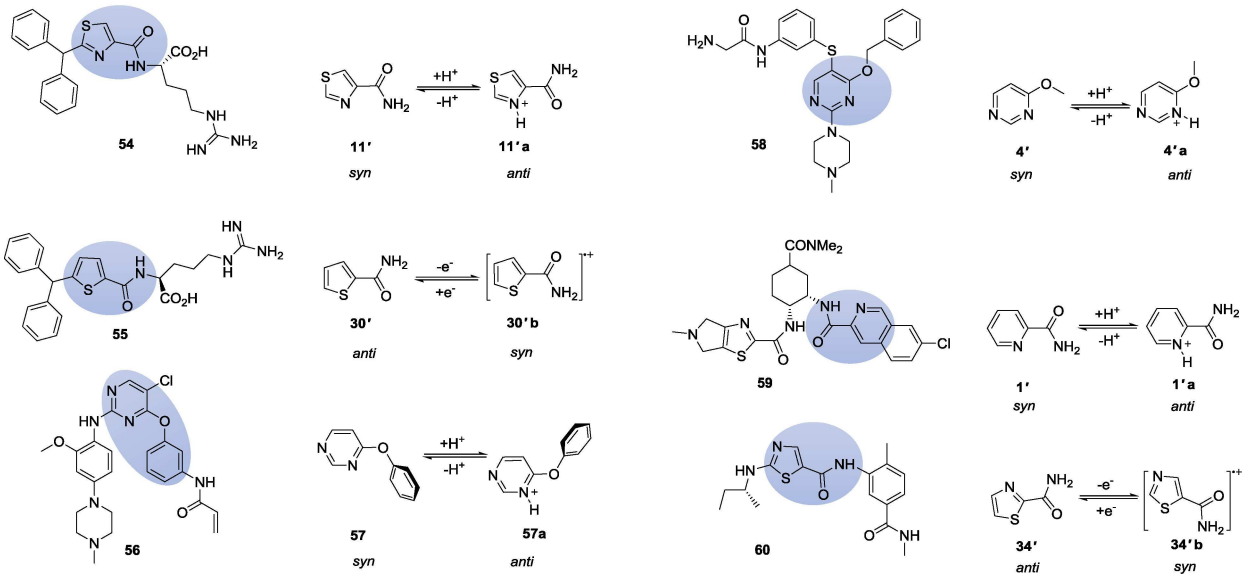

Figure 5. The potential effects of protonation and ionization on the conformations of drugs. (a) the C3a agonist **54** and the protonation effect on conformational preference of 1,3-thiazole-4-carboxamide **11**′; (b) the C3a antagonist **55** and the ionization induced conformational switching of 2-thiophenylcarboxamide **30**′; (c) the EGFR inhibitor **56** and the pH-triggered conformational switching of ether **57** (substructure of compound **56**), (d) Hsp70, (e) factor Xa, (f) MAP kinase inhibitor.

logical function of drugs by dramatically influencing complementarity between drug and receptor. Understanding key factors determining conformation will help to select heteroaromatic templates for elaboration in drug discovery and performance. For the recently developed C3a agonist/antagonist[7] (compounds **54** and **55**) from different conformers or several kinds of inhibitors[30–32] (EGFR **56**, Hsp70 **58**, factor Xa **59** and MAP kinase inhibitor **60**) containing structures similar to *o*-heteroaromatic ethers or amides, the pH or redox effect should be taken into account in their design or function (Figure 5). Additionally, the conformational fixation of amide has been used as a new synthetic method, in the ring-closing metathesis to yield medium-sized lactams.[33]

The protonation induced conformational switching can also be applied in the experiments of molecular recognition.[27] The combination of *2-[6]1N* **1** and adenine **61** was found to occur at low pH, as the electrostatic surfaces of *2-[6]1N* **1**/*2-[6]1NH*$^+$ **1a** conformers and adenine shown in Figure 6, the preferred *anti* conformer of *2-[6]1NH*$^+$ **1a** is more suitable for combination with adenine **61** through two hydrogen bonds to simulate the

© 2019 The Authors. Published by Wiley-VCH Verlag GmbH & Co. KGaA

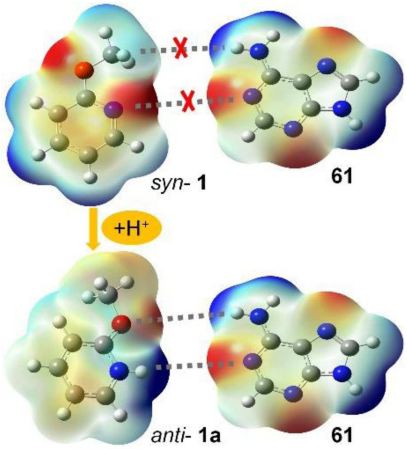

Figure 6. Electrostatic surfaces of 2-[6]1N **1**/2-[6]1NH$^+$ **1 a** conformers and adenine **61**.

nucleic acid base pair (A–T) than the preferred *syn* conformer of *2-[6]1N* **1**.

3. Discussion

3.1. About the Origin of Conformational Preferences

The *anti*-preferring protonated states and *syn*-preferring ionized states may provide critical information for understanding the origin of conformational preferences. The steric,[2] quantum[3] and electrostatic effects[5,6,11] have long been related to the origin of conformational preferences and bond rotational barrier, although there are still controversies about which factor is more important. For the ethane-like molecules, such as ethane, methylamine, methanol and hydrazine, the two energy partition schemes[5] revealed that the electrostatic interaction determines the barrier height (conformational stability) even though the steric effects and orbital interactions play indispensable roles. For the *o*-heteroaromatic ethers and amides which are much more complicated than ethane-like[1–3,5] small molecules, Chien and Corey considered the electronic repulsion between lone-pairs of electrons as the determining factor of conformational preferences of *o*-heteroaromatic ethers,[11] while Reid *et al.* reported that the stereoelectronic effects exerted by heteroatom dictate the conformation of heterocyclic amides.[6] Although both the two reactions involve introducing a positive charge into a molecule, the protonated and ionized molecules are not isoelectronic, and their structures are different. For a molecule containing N electron and M nucleus, the ionized molecule has N−1 electron and M nucleus, while the protonated one has N electron and M+1 nucleus. According to the equilibrium thermodynamics, the protonated form has one more neutral hydrogen atom than the corresponding ionized one (ground state), which may account for the different effects of protonation or ionization on the conformational preference of o-heteroaromatic ethers and amides. In this section, the discussions starting from the charge population analysis will provide some unambiguous physical images on the origin of conformational preferences. A qualitative analysis of electrostatic effect is firstly conducted with some typical compounds, then followed by quantitative analyses of steric and quantum effects.

3.2. Electrostatic Interactions Between OCH_3 and Ring

Figure 7 displays the partial natural population analysis (NPA) charges on atoms of OCH_3 group and two *ortho* positions. As

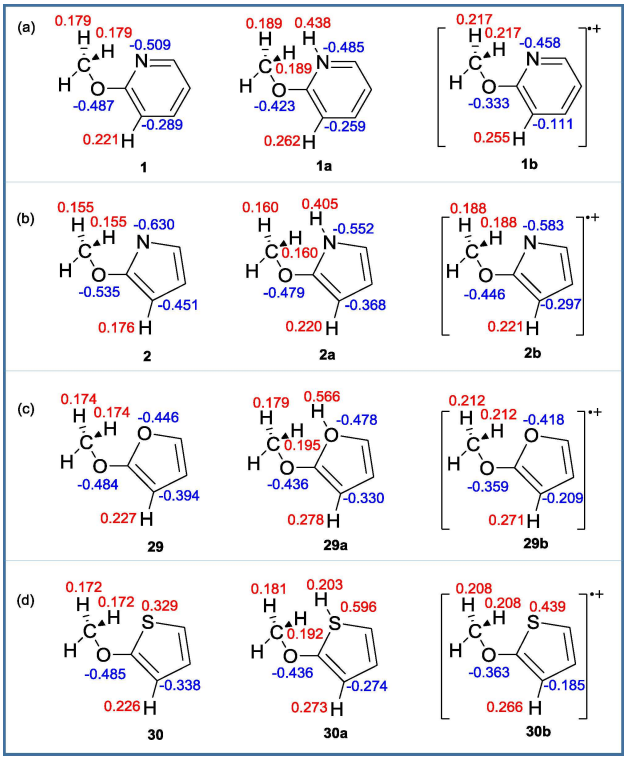

Figure 7. Partial NPA charges on OCH_3 and *ortho*-positions of the *syn* conformers of (a) 2-[6]1N **1**, (b) 2-[5]1N$^-$ **2**, (c) 2-[5]1O **29** and (d) 2-[5]1S **30** together with their protonated and ionized states.

shown in Figure 7(a), the positive charges on the H_{methyl} atoms in compounds *2-[6]1N* **1** and *2-[6]1NH*$^+$ **1 a** are +0.179 and +0.189, respectively. Correspondingly, the *ortho*-H_{aryl} atoms are also positively charged (+0.221 for *2-[6]1N* **1** and +0.262 for *2-[6]1NH*$^+$ **1 a**). On the other side of OCH_3, the charge on *ortho*-N heteroatom is determined to be −0.509 in *2-[6]1N* **1** and −0.485 in *2-[6]1NH*$^+$ **1 a**, while the charge on the introduced proton is +0.438 in *2-[6]1NH*$^+$ **1 a**, which shows that, upon protonation, the introduced positive charge is mainly populated on the proton connecting to the *ortho*-N heteroatom. For the protonated ether *2-[6]1NH*$^+$ **1 a**, the electrostatic repulsion[6,11] between the introduced positive proton (+0.438) and the positive H_{methyl} atoms of OCH_3 group (+0.189) will significantly make the *syn* conformers unstable. Similar results are also found in Figures 7(b)–(c). For *2-[5]1SH*$^+$ **30 a** shown in Figure 7(d), the

© 2019 The Authors. Published by Wiley-VCH Verlag GmbH & Co. KGaA

Table 4. Effects of exchange repulsion and delocalization.[a]

Numbers	Compounds	ΔE_{ex}	$\Delta E_{p-\pi^*}$	ΔE_{Hyper}	ΔE_{deloc}	ΔE_{sum} [b]	ΔE [c]
1	2-[6]1N	−0.47	4.92	1.65	6.57	6.10	4.08
2	2-[5]1N$^-$	−0.20	−0.89	1.44	0.55	0.35	1.68
29	2-[5]1O	0.55	−2.09	0.05	−2.04	−1.49	−1.14
30	2-[5]1S	0.88	−3.56	0.27	−3.29	−2.41	−0.92
1b	2-[6]1N$^+$	−1.02	3.68	2.58	6.26	5.24	6.22
2b	2-[5]1N$^\bullet$	−0.15	2.34	2.23	4.57	4.42	3.91
29b	2-[5]1O$^+$	−0.05	0.19	0.93	1.12	1.07	1.58
30b	2-[5]1S$^+$	−0.10	−0.33	0.86	0.53	0.43	0.62

[a] Calculated at ωB97XD/cc-pVTZ level. [b] $\Delta E_{sum} = \Delta E_{ex} + \Delta E_{p-\pi^*} + \Delta E_{Hyper}$. [c] Energy differences between *syn* and *anti* conformer.

ortho-S heteroatom becomes more positive upon protonation, indicating that the introduced positive charge is mainly populated on *ortho*-S instead of the proton itself, which will also destabilize the *syn* conformer. Additionally, another indispensable factor supporting the *anti* preferences of protonated ethers is the spatial or steric effects, due to the increased crowdedness caused by the protonation on the *o*-heteroatoms. However, the quantitative analysis below indicates that the steric effect seems not the determinant.

The other reaction introducing a positive charge is ionization. The positive charges on the H_{methyl} (+0.217 for *2-[6]1N*$^+$ **1b**) and *ortho*-H_{aryl} (+0.255 for *2-[6]1N*$^+$ **1b**) atoms are increased upon ionization, and the increased electrostatic repulsion between them will destabilize the *anti* conformers. While the negative charge on *ortho*-C is remarkably decreased upon ionization, and the electrostatic attraction between it and the positive H_{methyl} will be weakened, which also destabilize the *anti* conformers. For the *ortho*-heteroatoms, as shown in Figures 7(a)-(c), these *o*-heteroatoms become slightly less negative upon ionization (−0.458 for *2-[6]1N*$^+$ **1b**, −0.583 for *2-[5]1N*$^\bullet$ **2b** and −0.418 for *2-[5]1O*$^+$ **29b**), and the decreased attractive interactions with H_{methyl} are still the supporting factor for the *syn* preferences observed in these ionized compounds. However, as shown in Figure 7(d), the positive charge on *ortho*-S is increased upon ionization, and the repulsive interaction with H_{methyl} is against the *syn* preferences of *2-[5]1S*$^+$ **30b**. The quantitative analysis below shows that, due to the decreased negative charge on ether-O atom, the delocalization effects dominate the *syn* preferences of *2-[5]1S*$^+$ **30b**. As shown in Figure 7(a)-(d), the negative charge on ether-O atom is remarkably decreased upon ionization.

It seems that the population of the introduced positive charge in a molecule can to some extent determine the conformational preferences. For the protonated compounds, the introduced positive charge is mainly located on the proton or the *ortho*-heteroatom, due to the increased repulsion between H_{methyl} and proton, the protonated molecule will be *anti*-preferring. While for the ionized compounds, the population of the introduced positive charge on the ether-O, H_{methyl} and *ortho*-H_{aryl} may play important roles in determining the *syn* preference. These findings rationalize the effects of protonation and ionization on conformational preferences. However, it seems that, especially for few neutral compounds containing *ortho*-O heteroatom, the conformational preferences cannot be interpreted only by the electrostatic interactions. For instance, the attraction between the positive H_{methyl} (+0.174) and the negative hetero-O atom (-0.446) does not support the *anti* preference of 2-[5]1O **29**. While the electronic repulsion between lone-pairs of electrons of the ether-O atom (-0.484) and hetero-O atom[6] also destabilize the *anti* conformer of 2-[5]1O **29**. Similarly, as shown in Figure 7(d), the strong repulsion between the positive H_{methyl} (+0.208) and the positive hetero-S atom (+0.439) is contradictory to the *syn* preference of 2-[5]1S$^+$ **30b**. In fact, besides of the electrostatic factor, it has been found that the repulsion and steric effects within molecules[34,35] act in similar way but cause quite opposite effects. So, the steric and quantum factors also need to be considered.

3.3. Steric and Orbital Interactions

The labeling for each atom of *2-[6]1N* **1**, *2-[5]1N*$^-$ **2**, *2-[5]1O* **29** and *2-[5]1S* **30** are shown in Figure S9. The pairwise steric exchange energy approximates the steric exchange interaction between two semi-localized natural localized molecular orbitals (NLMOs). And the steric exchange energy (ΔE_{ex}) between OCH_3 group and the ring are approximately described by the summation of the pairwise energy terms, which are related to the orbitals nearby OCH_3 group. For the conjugation ($\Delta E_{p-\pi^*}$) and hyperconjugation (ΔE_{Hyper}) effects, energies are obtained by examining all possible interactions between "filled" Lewis-type NBOs (donor) and "empty" non-Lewis NBOs (acceptor) with the aid of second-order perturbation theory. The detailed energetic components for exchange repulsion, p-π* conjugation and hyperconjugation are tabulated in Tables S5–S10. Here, only the summarized results of energy differences are shown in Table 4.

The calculated differences in steric exchange repulsion[36] and delocalization between the *syn* and *anti* conformers (Table 3) show that, for the ethers and ionized ethers, the ΔE_{deloc} values have the same tendency with respect to those of ΔE_{sum} and conformational energy differences, ΔE. While the steric exchange repulsion term, ΔE_{ex}, are mostly smaller than 1.0 kcal/mol and the tendencies are not in agreement with ΔE. Particularly, for compound **30b**, the conformational energy differences, ΔE (+0.62 kcal/mol), can be approximately described by ΔE_{deloc} (+0.53 kcal/mol) instead of the ΔE_{ex}

© 2019 The Authors. Published by Wiley-VCH Verlag GmbH & Co. KGaA

(−0.10 kcal/mol). Similar results can be found for compounds **29** and **30** where the determining term is ΔE_{deloc} (−2.04 and −3.29 kcal/mol for *2-[5]1O* **29** and *2-[5]1S* **30**, respectively). While the sign of ΔE_{ex} (0.55 kcal/mol for compound **29** and 0.88 kcal/mol for compound **30**) is opposite to those of ΔE (−1.14 and −0.92 kcal/mol for compounds **29** and **30**, respectively). These findings show that the delocalization effects[3,4] are the supporting and determining factor of conformational preferences of neutral compounds containing *ortho*-O or S atom (**29**–**36**). While the steric exchange repulsion seems relatively unimportant, which can be either a supporting factor or not. So, in combination with the electrostatic analysis, it shows that both the orbital interactions and the electrostatic attractions are main stabilizing factors to the *syn* or *anti* preferences. On the other hand, the destabilizing factors are determined by the electrostatic repulsion instead of the steric exchange repulsion between OCH_3 group and the ring. Certainly, there are still some questionable disadvantages in these natural bond orbital analyses leading to some deviations, such as the incomplete orbital selection, the omitted electrostatic contributions, etc. Undoubtedly, more detailed theoretical investigations are helpful for clarifying the origin of conformational preferences of these *ortho*-substituted heteroarenes.

3.4. Weak Interactions – an IGM Analysis

To provide a more unambiguous physical image on the origin of conformational preferences and switching, the interfragment interactions between the substituent and heteroaromatic ring were investigated by performing IGM analysis. The IGM proposed by Lefebvre *et al.*,[37] is a very useful methodology to study interfragment and intrafragment interactions by using pro-molecular density. Briefly, only some essential idea of this method is outlined in the most general forms. To study the interfragment interactions, two important functions, $g^{IGM,inter}$ and g^{inter}, are defined in the equations (1) and (2), respectively (Scheme 1). The g^{inter} represents the sum of density gradient

$$g^{inter}(\mathbf{r}) = \left| \sum_{A} \sum_{i \in A} \nabla \rho_i(\mathbf{r}) \right| \quad (1)$$

$$g^{IGM,\,inter}(\mathbf{r}) = \left| \sum_{A} \mathrm{abs}\left[\sum_{i \in A} \nabla \rho_i(\mathbf{r}) \right] \right| \quad (2)$$

$$\delta g^{inter}(\mathbf{r}) = g^{IGM,inter}(\mathbf{r}) - g^{inter}(\mathbf{r}) \quad (3)$$

Scheme 1. Definitions of the $g^{IGM,inter}$ and g^{inter} functions.

$(\nabla \rho_i(\mathbf{r}))$ of each atom in their free states, where the i and A are index of atoms and fragments, respectively. While $g^{IGM,inter}$ is the IGM type of gradient, which is calculated as sum of the absolute value of $\nabla \rho_i(\mathbf{r})$. Noting that the $g^{IGM,inter}$ is the upper limit of g^{inter}, and a new descriptor δg^{inter} uniquely defining the intermolecular interaction regions can be derived as the difference between $g^{IGM,inter}$ and g^{inter} (equation (3)).

The term $sign(\lambda_2)\rho(r)$ represents the product of electron density ρ(r) and sign of the second eigenvalue of electron-density Hessian matrix, and can be mapped to δg^{inter} isosurfaces by different colors to detect the regions as well as the characters (repulsive or attractive) of the weak interactions.

Figure 8 displays the results of the IGM analysis for some typical compounds **1**, **30**, **1′** and **30′** together with their corresponding protonated and ionized forms. As shown in graph (a) of Figure 8, for the neutral *anti* conformers, the isosurfaces are filled by green to red, revealing that the interactions in these regions are mainly repulsive. While for the *syn* conformers, the properties of the interactions in neutral compounds **1** and **1′** are remarkably different from those in the compounds **30** and **30′**. Particularly, the interfragment interactions between substituent (OCH_3 or $CONH_2$) and pyridine are explicitly attractive. While in the case of compounds **30** and **30′**, the isosurfaces in these regions are mainly colored by green, revealing a very weak attractions. These differences support the results listed in Tables 1 and 2, i.e., the compounds **1** and **1′** are *syn* preferred while the two thiophene derivatives (compounds **30** and **30′**) are slightly *anti* preferred.

For protonation, since our attention are mainly focused on the protonation on *ortho*-N heteroatom and only some estimated values (without ZPCs) are available for compound **30a**, here only the results of compounds **1a** and **1′a** are exhibited in Figure 8(b). For the *anti* conformers, there are still moderate repulsions between the substituent and the ring. Comparing with the unprotonated *syn* conformers in Figure 8(a), the blue regions in *syn 2-[6]1NH*$^+$ **1a** and *2′-[6]1NH*$^+$ **1′a** are remarkably smaller than those in the neutral *2-[6]1N* **1** and *2′-[6]1N* **1′**, indicating the weaker attractions in these protonated *syn* conformers. While the red areas are increased in these two protonated *syn* conformers, which coincides with the protonation-induced conformational switching as shown in Tables 1 and 2.

As shown in Figure 8(c), the interactions in *anti 2-[6]1N*$^+$ **1b** are slightly more repulsive than that in *anti 2-[6]1N* **1**, while the strength of attractive interactions in *syn 2-[6]1N*$^+$ **1b** is similar to the neutral form, revealing the enhanced *syn* preference upon ionization. In the case of compound **30**, the red or orange isosurface between OCH_3 and *ortho*-S heteroatom in *syn* 2-[5]1S **30** is slightly decreased upon ionization, indicating a decreased repulsion. These changes are not remarkable in the amide **30′**, which coincides with the weak conformational preferences listed in Table 2. For the *2′-[6]1N*$^+$ **1′b** cation, it is found that the attractive interaction region (blue region between NH_2 and *ortho*-N heteroatom) shrinks remarkably. This shrinking of attraction area may be attributed to the decreasing of negative charge on the *ortho*-N heteroatom upon ionization, which will weaken the N–H···N hydrogen bond. By using Espinosa's model (based on QTAIM data),[38,39] the energy of NH···N hydrogen bond in the molecule **1′** and **1′b** are determined to be −1.89 kcal/mol and −0.57 kcal/mol, respectively, revealing that upon ionization, the NH…N hydrogen bond has been weakened. This supports the above IGM analysis shown in Figure 8.

© 2019 The Authors. Published by Wiley-VCH Verlag GmbH & Co. KGaA

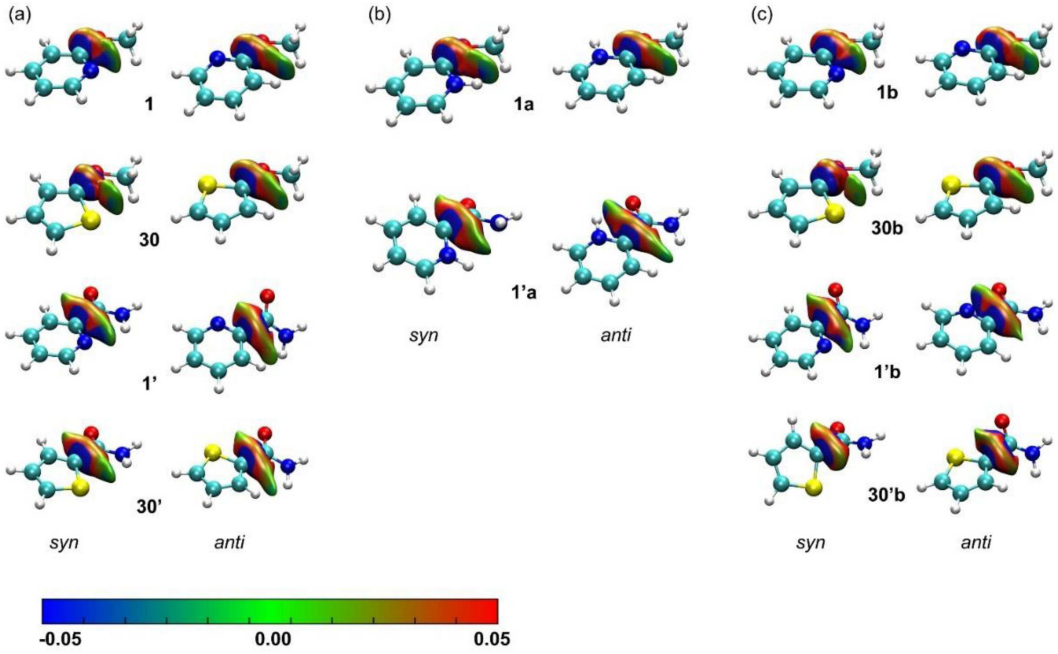

Figure 8. The plotting for the δg^{inter} isosurfaces of interfragment interactions between the OCH_3 and the heteroaromatic ring of (a) the neutral compounds, (b) the protonated forms and (c) the ionized forms. The isosurfaces for each conformers are color-filled by the blue-green-red (BGR) color scale method.

Investigators usually suggested some factor as the origin of conformational preferences.[5] However, it seems to us that, due to the diversities of molecular structures, the determining factor for conformational preference might be different for different molecular systems. Considering the analysis of NPA charge, steric and orbital interactions, the repulsion between substituent (OCH_3 or $CONH_2$) and heteroaromatic ring is probably dominated by electrostatic repulsion instead of the relatively unimportant steric repulsion. While both the electrostatic and orbital interactions (via conjugation and hyperconjugation) might be responsible for the interfragment attractions. As for the protonated and ionized *o*-heteroaromatic ethers and amides, the electrostatic effect can mainly account for the conformational preferences, which is in agreement with the earlier studies on several neutral ethane-like molecules. Intrinsically, it is the difference in reactive sites between protonation (introducing a positive H^+) and ionization (removing an electron) that is responsible for the origin of different effects on conformational preferences. Upon protonation or ionization, the resultant conformational preferences are mainly determined by charge distribution in the molecules, which might simultaneously affect the electrostatic and orbital interactions.

4. Conclusions

The positive charge introduced by protonation or ionization has strong effects on the conformaional preferences of *o*-heteroaromatic ethers and amides, providing potential methods for conformation control. Calculations reveal that, although these ethers and amides have not only *syn* preferences for those containing an *ortho*-N heteroatom but also *anti* preferences for those containing *ortho*-O or S heteroatom, all the protonated ethers or amides are *anti* preferring but all the ionized ones are *syn* preferring. Difference in population of the positive charge introduced by protonation or ionization can mainly account for the different effect on conformation. The determining factor of conformational preference is the electrostatic interaction for the protonated compounds and most of the ionized compounds, but the orbital interactions for those ionized compounds containing *ortho*-S heteroatom. Since the conclusions are based on the complete inductive method, they could be considered as rules for conformational preferences of these ethers and amides. The protonation and ionization could be easy and applicable ways to modulate the conformers of monocyclic *o*-heteroaromatic ethers or amides, by pH control and oxidation. In virtue of its two conformation, the aromatic ether oxygen or amide bonds can operate to orient a chain in conformational space, and the strong conformational preferences and switching can be harnessed for the design of functional molecules and modification of molecular biological process.

Experimental Section

Computational Methods

The geometrical structures of all the studied ethers and amides are optimized at ωB97XD/cc-pVTZ[20,21] level, which is followed by frequency calculations to obtain zero point corrections (ZPCs). All the values of the conformational energy differences are derived from the expression, $\Delta E = E_{anti} - E_{syn}$. Some data are marked with alphanumeric numbering, which represent the single point energy differences between *syn* and *anti* conformers, due to the failures of convergence during geometry optimizations or self-consistent field

© 2019 The Authors. Published by Wiley-VCH Verlag GmbH & Co. KGaA

(SCF) calculations. All the calculated energy values are confirmed by a high precision method Gaussian-4 (G4),[40] which are shown in Table S4. The potential curves are calculated by relaxed scan at ωB97XD/cc-pVTZ level. Without ZPCs, the conversion barriers between *syn* and *anti* conformers are obtained from these potential curves. The exchange repulsion and delocalization (Here, the delocalization effect (ΔE_{deloc}) includes p-π* conjugation ($\Delta E_{p\text{-}\pi^*}$) and σ-σ* hyperconjugation (ΔE_{Hyper}) nearby the OCH_3 group are calculated by using the stand-alone NBO 5.0 program.[41] The Independent Gradient Model (IGM)[37] is employed to visually explore the interfragment interactions, which is performed by using Multiwfn package[42] and the Visual Molecular Dynamics (VMD) program.[43]

R2PI Spectroscopic Experiment

The 2-[6]1N (2-methoxypyridine, b.p. 142–143 °C) sample with a purity of 99% was purchased from Acros Corporation, which was used without further purification and seeded in the Ar carrier gas (ca. 2.5 atm) at room temperature (ca. 298 K). To generate a supersonic molecular beam, the sample seeded Ar gas was expanded into the vacuum chamber (source chamber, ca. 3.0×10^{-3} Pa) through a pulsed valve (General valve series 9, diam. 0.25 mm). Then the molecular beam was collimated by a skimmer (diam. 1 mm) before entered the ionization chamber (ca. 3.0×10^{-5} Pa).

The home-built R2PI experimental system has been described in our previous publication.[44] Briefly, in the 1C-R2PI spectroscopic experiment, the molecular beam interacted perpendicularly with one UV laser beam to obtain the ionized sample molecules, which can be successively accelerated by two DC electric fields of 200 and 3500 $V\cdot cm^{-1}$. After being focused by einzel lens, these accelerated cations entered into a 1.0 meter-long field-free tube.

The cations were detected by a dual-stacked micro-channel plate (MCP) detector. Then the signals were amplified through a pre-amplifier (Stanford Research System, SR445A) and collected by a multi-channel scaler (MCS, Stanford Research system, SR430) and transported to the data collection terminal. By using a pulse delay generator (DG535, Stanford Research System), the sequential control of the whole system was achieved. Usually, the excitation energies of the conformers coexisting in a sample may only differ by a few hundreds of wavenumbers. To obtain a vibronic spectrum with high resolution, the step size of scanning job was set to 0.04 nm/step (ca. 2.5 cm^{-1}/step) and each point was accumulated for 300 laser shots to counteract the fluctuation of laser power.

Pumped by a Nd:YAG laser at the frequency of 10 Hz, a tunable dye laser (Sirah Dye Laser-CSTR) provided the UV laser radiation in the R2PI experiment. In the present work, Coumarin 153 and Pyrromethene 597 dyes were used.

Acknowledgements

We gratefully acknowledge the financial support from the National Natural Science Foundation of China under Grants No. 20973180 and 21190034. The theoretical calculations were mainly performed on the China Scientific Computing Grid (ScGrid) of the Supercomputing Center, Computer Network Information Center of the Chinese Academy of Sciences.

Conflict of Interest

The authors declare no conflict of interest.

Keywords: conformational modulation · heteroaromatic ethers · heteroaromatic amides · protonation · ionization

[1] F. Weinhold, *Nature* **2001**, *411*, 539–541.
[2] F. M. Bickelhaupt, E. J. Baerends, *Angew. Chem. Int. Ed.* **2003**, *42*, 4183–4188; *Angew. Chem.* **2003**, *115*, 4315–4320.
[3] V. Pophristic, L. Goodman, *Nature* **2001**, *411*, 565–568.
[4] Y. R. Mo, *Nat. Chem.* **2010**, *2*, 666–671.
[5] S. B. Liu, *J. Phys. Chem. A* **2013**, *117*, 962–965.
[6] R. C. Reid, M.-K. Yau, R. Singh, J. Lim, D. P. Fairlie, *J. Am. Chem. Soc.* **2014**, *136*, 11914–11917.
[7] R.-J. Lohman, J. K. Hamidon, R. C. Reid, J. A. Rowley, M.-K. Yau, M. A. Halili, D. S. Nielsen, J. Lim, K.-C. Wu, Z. Loh *Nat. Commun.* **2017**, *8*, 351.
[8] K. P. Lu, G. Finn, T. H. Lee, L. K. Nicholson, *Nat. Chem. Biol.* **2007**, *3*, 619–629.
[9] M. McTigue, B. W. Murray, J. H. Chen, Y.-L. Deng, J. Solowiej, R. S. Kania, *Proc. Natl. Acad. Sci. USA* **2012**, *109*, 18281–18289.
[10] A. Kondoh, Y. Ota, T. Komuro, F. Egawa, K. Kanomata, M. Terada, *Chem. Sci.* **2016**, *7*, 1057–1062.
[11] R. J. Chein, E. J. Corey, *Org. Lett.* **2010**, *12*, 132–135.
[12] C. Siebler, B. Maryasin, M. Kuemin, R. S. Erdmann, C. Rigling, C. Grünenfelder, C. Ochsenfeld, H. Wennemers, *Chem. Sci.* **2015**, *6*, 6725–6730.
[13] H. Asami, S.-H. Urashima, M. Tsukamoto, A. Motoda, Y. Hayakawa, H. Saigusa, *J. Phys. Chem. Lett.* **2012**, *3*, 571–575.
[14] D. Mazzier, M. Crisma, M. De Poli, G. Marafon, C. Peggion, J. Clayden, A. Moretto, *J. Am. Chem. Soc.* **2016**, *138*, 8007–8018.
[15] S. Amirjalayer, A. Martinez-Cuezva, J. Berna, S. Woutersen, W. Jan Buma, *Angew. Chem. Int. Ed.* **2018**, *57*, 1792–1796; *Angew. Chem.* **2018**, *130*, 1810–1814.
[16] E. J. Cocinero, P. Çarçabal, T. D. Vaden, J. P. Simons, B. J. Davis, *Nature* **2011**, *469*, 76–80.
[17] W. Viricel, A. Mbarek, J. Leblond, *Angew. Chem. Int. Ed.* **2015**, *54*, 12743–12747; *Angew. Chem.* **2015**, *127*, 12934–12938.
[18] W. S. Dai, S. Liu, Z. Zhang, X. P. Chi, M. Cheng, Y. K. Du, Q. H Zhu, *Phys. Chem. Chem. Phys.* **2018**, *20*, 6211–6226.
[19] I. M. Jones, P. C. Knipe, T. Michaelos, S. Thompson, A. D. Hamilton, *Molecules* **2014**, *19*, 11316–11332.
[20] J.-D. Chai, M. Head-Gordon, *Phys. Chem. Chem. Phys.* **2008**, *10*, 6615–6620.
[21] R. A. Kendall, T. H. Dunning, Jr., R. J. Harrison, *J. Chem. Phys.* **1992**, *96*, 6796–6806.
[22] M. J. Frisch, G. W. Trucks, H. B. Schlegel, G. E. Scuseria, M. A. Robb, J. R. Cheeseman, G. Scalmani, V. Barone, B. Mennucci, G. A. Petersson *Gaussian 09*, Revision C.01; Gaussian Inc.: Wallingford CT, **2010**.
[23] W. J. P. Blonski, F. E. Hruska, T. A. Wildman, *Org. Magn. Reson.* **1984**, *22*, 505–509.
[24] R. Yamasaki, A. Tanatani, I. Azumaya, S. Saito, K. Yamaguchi, H. Kagechika, *Org. Lett.* **2003**, *5*, 1265–1267.
[25] A. L. Bartuschat, K. Wicht, M. R. Heinrich, *Angew. Chem. Int. Ed.* **2015**, *54*, 10294–10298; *Angew. Chem.* **2015**, *127*, 10433–10437.
[26] U. J. Lorenz, J. Lemaire, P. Maitre, M.-E. Crestoni, S. Fornarini, O. Dopfer, *Int. J. Mass Spectrom.* **2007**, *267*, 43–53.
[27] I. Novosjolova, S. D. Kennedy, E. Rozners, *ChemBioChem* **2017**, *18*, 2165–2170.
[28] L. J. Zhang, S. Liu, M. Cheng, Y. K. Du, Q. H. Zhu, *J. Phys. Chem. A* **2016**, *120*, 81–94.
[29] M. Head-Gordon, J. A. Pople, M. J. Frisch, *Chem. Phys. Lett.* **1988**, *153*, 503–506.
[30] H. Cheng, S. K. Nair, B. W. Murray, C. Almaden, S. Bailey, S. Baxi, D. Behenna, S. Cho-Schultz, D. Dalvie, D. M. Dinh, et al, *J. Med. Chem.* **2016**, *59*, 2005–2024.
[31] L. Wang, J. Zhao, Y. Yao, C. Wang, J. Zhang, X. Shu, X. Sun, Y. Li, K. Liu, H. Yuan, X. Ma, *Eur. J. Med. Chem.* **2017**, *142*, 493–505.
[32] B. R. Beno, K.-S. Yeung, M. D. Bartberger, L. D. Pennington, N. A. Meanwell, *J. Med. Chem.* **2015**, *58*, 4383–4438.

© 2019 The Authors. Published by Wiley-VCH Verlag GmbH & Co. KGaA

[33] N. Hegmann, L. Prusko, N. Diesendorf, M. R. Heinrich, *Org. Lett.* **2018**, *20*, 7825–7829.
[34] B. Ośmiałowski, E. Kolehmainen, M. Kowalska, *J. Org. Chem.* **2012**, *77*, 1653–1662.
[35] B. Ośmiałowski, E. Kolehmainen, S. Ikonen, A. Valkonen, A. Kwiatkowski, I. Grela, E. Haapaniemi, *J. Org. Chem.* **2012**, *77*, 9609–9619.
[36] J. K. Badenhoop, F. Weinhold, *J. Chem. Phys.* **1997**, *107*, 5406–5421.
[37] C. Lefebvre, G. Rubez, H. Khartabil, J.-C. Boisson, J. Contreras-García, E. Hénon, *Phys. Chem. Chem. Phys.* 2017, 19, 17928–17936.
[38] E. Espinosa, E. Molins, C. Lecomte, *Chem. Phys. Lett.* **1998**, *285*, 170–173.
[39] E. Espinosa, M. Souhassou, H. Lachekar, C. Lecomte, *Acta Crystallogr. Sect. B* **1999**, *55*, 563–572.
[40] L. A. Curtiss, P. C. Redfern, K. Raghavachari, *J. Chem. Phys.* **2007**, *126*, 084108.
[41] E. D. Glendening, J. K. Badenhoop, A. E. Reed, J. E. Carpenter, J. A. Bohmann, C. M. Morales, F. Weinhold, *NBO 5.0*, Theoretical Chemistry Institute, University of Wisconsin, Madison, WI, **2001**.
[42] T. Lu, F. Chen, *J. Comput. Chem.* **2012**, *33*, 580–592.
[43] W. Humphrey, A. Dalke, K. Schulten, *J. Mol. Graphics* **1996**, 14, 33–38.
[44] D. Q Xiao, D. Yu, X. L. Xu, Z. J. Yu, Y. K. Du, Z. Gao, Q. H. Zhu, C. H. Zhang, *J. Mol. Struct.* **2008**, *882*, 56–62

Manuscript received: March 21, 2019
Revised manuscript received: May 6, 2019

© 2019 The Authors. Published by Wiley-VCH Verlag GmbH & Co. KGaA